Spectral modulation and supercontinuum generation assisted by infrared femtosecond plasma grating*

Liu Zuo-Ye(刘作业), Sun Shao-Hua(孙少华), Shi Yan-Chao(史彦超), Ding Peng-Ji(丁鹏基), Liu Qing-Cao(刘情操), Liu Xiao-Liang(刘小亮), Ding Bao-Wei(丁宝卫), and Hu Bi-Tao(胡碧涛)†

School of Nuclear Science and Technology, Lanzhou University, Lanzhou 730000, *China*

(Received 22 November 2012; revised manuscript received 16 January 2013)

Spectral modulation and supercontinuum generation of a probe pulse is investigated by using the plasma grating induced by the interference of two infrared femtosecond laser pulses. The dependences of the supercontinuum generation from the probe pulse on the time delay, the relative polarization angle between the probe pulse and the two-pump pulses, and the input probe pulse energy are investigated. The far-field spatial profiles of the three pulses are measured with different time delays and relative polarization angle, and the core energy of the probe pulse as functions of the time delay and relative polarization angle are also shown.

Keywords: plasma grating, supercontinuum generation, redistribution of refractive index

PACS: 52.38.Hb, 42.65.Re, 42.65.Jx **DOI:** 10.1088/1674-1056/22/7/075204

1. Introduction

Filamentation of femtosecond laser pulses[1–18] is a rich interdisciplinary branch of modern physics that deals with the propagation of ultra-intense laser pulses in transparent media. Filamentation with self-stabilized intensity clamping in self-guided channels owing to the dynamic balance between Kerr self-focusing and plasma defocusing, induces plenty of nonlinear optical phenomena, such as self-compression,[6–11] THz generation,[12–14] the third harmonic generation,[15,16] supercontinuum (SC) generation.[17,18] The SC generation with ultra-broadband spectra covering a spectral range from near infrared (IR) to ultraviolet (UV) was intensively investigated in different optical media[19–23] and stimulates important applications in various fields.[24–28] Several nonlinear processes, such as the self-phase modulation, four-wave mixing and self-steepening, are now understood to broaden the pulse spectrum and contribute to SC generation. The first SC generation with a spectral range from IR to UV was obtained by femtosecond-laser pulses propagating in high-pressure gases. Control and optimization of the filamentation characteristics are required for potential applications of the filamentation of femtosecond laser pulses. Various experiments were performed to study the spatial dynamics of filament formation in the air, including fusion and competition of multiple filaments. Recently, more refined methods to control the filamentation of a femtosecond laser pulse were introduced. One is using an optical airy beam to form a curved trajectory of the filament in the air and water.[29,30] Another method relies on the molecular lensing: the probe filament can be sucked into the pump filament's molecular quantum wake and trapped or destroyed by it.[31] For diatomic molecules, the filamentation dynamics are well controlled by the alignment and the rotational states of molecules, and the SC cut-off wavelength in the UV spectral range are controlled by using the quantum wake of impulsive molecular alignment through filamentation of a femtosecond laser pulse with a longer temporal duration and more moderate driving intensity.

The plasma grating[32,33] generated by noncollinear interaction of multiple IR femtosecond filaments exhibits captivating properties for further research. The laser power density inside the plasma grating may be beyond the clamping intensity limit for a single filament,[34–36] and the peak electron density inside the plasma grating was demonstrated to be two orders of magnitude higher than that inside a single femtosecond filament.[28] By using a UV plasma grating, Bragg diffraction efficiency was used to estimate the free-electron density inside the interaction area. A plasma grating was also applied to study the laser energy exchange between the two femtosecond filaments forming the plasma grating.[26,27] Recently, we studied the enhancement and spectral broadening of the third harmonic generated from a third probe pulse by a plasma grating.[37]

As plasma gratings show so many fascinating characteristics, the spectral modulation and the SC generation of a probe pulse are investigated by using a femtosecond plasma grating in this paper. The probe femtosecond pulse is focused on the plasma grating with a small crossing angle, and the SC from the probe pulse and spatial profiles of the three pulses are measured. The dependences of the SC generation and the core energy of probe pulse on the time delay and the relative polar-

*Project supported by the National Natural Science Foundation of China (Grant Nos. 11135002, 11075069, 91026021, and 11075068) and the Scholarship Award for Excellent Doctoral Student of Ministry of Education, China.

†Corresponding author. E-mail: hubt@lzu.edu.cn

© 2013 Chinese Physical Society and IOP Publishing Ltd

ization angle between the probe pulse and the pump pulses are investigated.

2. Experimental setup

The experiment was performed using a Ti:Sapphire chirped-pulse amplification laser system (1 kHz, 810 nm, and 33 fs). The experimental schematic is shown in Fig. 1(a). Two pulses with pulse energy up to 0.7 mJ and 0.8 mJ were focused to form a plasma grating by using two 63-cm-focal-length lens. The probe pulse with pulse energy up to 0.6 mJ was focused to form a longer filament with length of about 2.5 cm by using a 110-cm-focal-length lens. The crossing angle θ was set to 3.8° while the angle ϕ was set to 3.5°. The fluorescence distributions of the interaction area could be recorded by a sensitive charge-coupled device (CCD) camera. A fused silica lens was used to focus the SC generated from the probe pulse into a fiber-pigtailed spectrometer (Ocean Optics, USB2000+) which was used to detect the spectra of the SC generation. We took the head of the fiber away and put a pinhole with a power meter into the beam pass to measure the core energy of the probe pulse. If all the components after the interaction area were moved away, the SC generation could directly irradiate a white screen. The distance between the white screen and the interaction area was about 60 cm. Then the output far-field profiles of the three pulses were recorded with a digital camera.

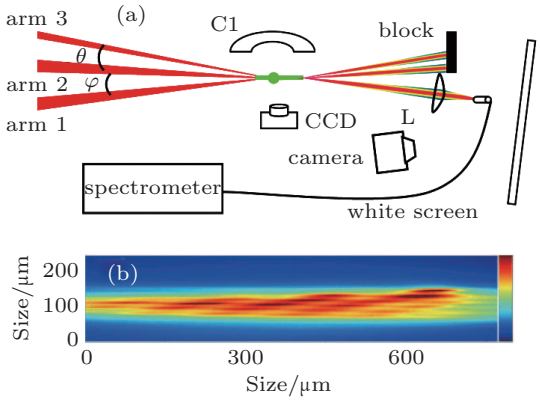


Fig. 1. (color online) (a) Schematic of the experimental setup for studying the dynamic of the probe pulse. The color bar represents the linear intensity scale inherent to the CCD camera. (b) The fluorescence distribution of the interaction area.

A plasma grating lasting several tens of picoseconds is formed when the time delay between the two pump pulses is 0 fs. The length of the plasma grating is about 700 μm and the spatial period Λ can be obtaned by the function $\Lambda = \lambda/2\sin(\theta/2)$. As shown in Fig. 1(b), the contrast ratio of the plasma grating is enhanced by the probe pulse, which was studied in our previous work.[37] The interaction length is enlarged, for the attraction between the probe pulse and the plasma grating, and the intensity of the fluorescence of the interaction area is improved up to ten times by the probe pulse, which means the enhancement of plasma density in the interaction area.

3. Experimental results and discussion

The dependence of the SC spectra of the probe pulse on the time delay is shown in Fig. 2(a). Figures 2(b)–2(g) show the output far-field spatial profiles of the three pulses measured with time delay of −10 ps (no interaction between the plasma grating and the probe pulse), −200 fs, −50 fs, 0 fs, 50 fs, and 200 fs, respectively. The time zero is defined as the time point when the fluorescence intensity of the interaction area is the highest and the negative delay means the probe pulse propagates ahead. As shown in Fig. 2(a), the output spectra of the probe pulse exhibit an obvious blue shift in the time range from −200 fs to 200 fs, and the cut-off wavelength of the SC spectrum is extended to 570 nm when the time delay is set to 0 fs. The intense interaction between two non-collinear filaments can induce the enhancement of the laser peak intensity of the interaction area due to the light filed interference.[28,35] The femtosecond laser pulse with higher energy produces more drastic competition[21] among the SC generation, multiphoton ionization losses, multifilamentation, and some other nonlinear processes. By tuning the time delay between the probe pulse and the pump pulses to be zero, an additional cross-defocusing effect is induced to loosen the focusing condition of the probe pulse. The cross-focusing effect can enhance the self-phase modulation, the self-steepening, space-time focusing effects, and the cross-phase modulation to broaden the SC spectrum of the probe pulse, resulting in the blue shift of the SC generation.[22] When the time delay between the probe pulse and pump pulses is set to be negative (temporal overlapping), the cross defocusing effect is progressively enhanced with the increase of the time delay. However, this effect is slightly suppressed with the increase of the time delay in the positive range, inducing the asymmetrical spectra of the SC generation detected with negative and positive time delay. As shown in Fig. 2(a), the output spectrum of the probe pulse obtained with negative time delay is wider than that obtained with positive time delay. The output spectra extend to about 610 nm and 600 nm with time delay of 200 fs and about 600 nm with time delay of −200 fs. Meanwhile, the intensity of broadening spectra obtained with negative time delay is higher than that obtained with positive time delay. It should point out that the possible reason for the suppression of the cross defocusing effect with positive time delay is multiphoton ionization loss.

Without interacting with the plasma grating, the self-cleaning core[38,39] of the probe pulse with the improvement of the spatial distribution in the far-field region is shown in Fig. 2(b). For the two-pump filament interaction with time delay between them set to 0 fs, bowlike diffraction of each pump

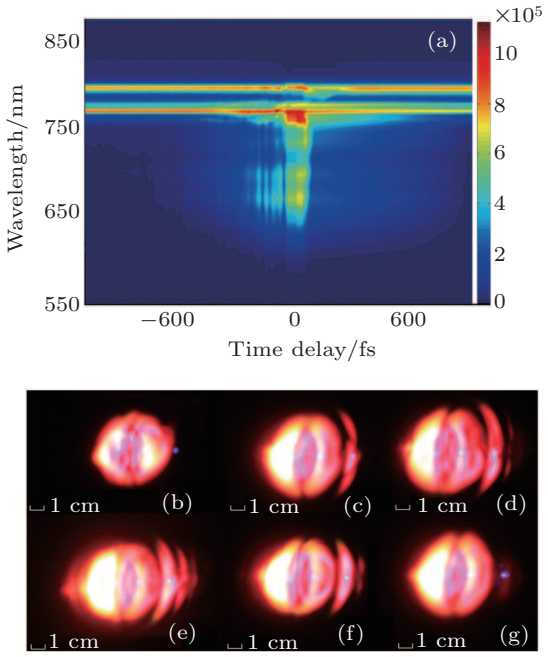


Fig. 2. (color online) (a) Dependence of measured SC spectra on time delay, and output spatial profiles of three pulses with different time delay between probe pulse and pump pulses. (b)–(g) are output spatial profiles with time delay of −10 ps (no interaction between plasma grating and probe pulse), −200 fs, −50 fs, 0 fs, 50 fs, and 200 fs, respectively.

pulse and threadlike fringes between them are observed in the far-field region. The bowlike diffraction of pump pulses is caused by the self-phase and cross-phase modulations, suggesting strong spatiotemporal couplings in the interaction area, while the threadlike fringes indicate self-guiding in the plasma grating.[39] With probe pulse interacting with the plasma grating, bowlike diffraction patterns of the two pump pulses are enlarged and threadlike fringes are deformed by the probe pulse, as shown in Figs. 2(c)–2(g). For the far-field profiles of the probe pulse, three bowlike patterns of the probe pulse are detected when the time delay is set to 0 fs. The frequency components distribute in different bowlike patterns are different, i.e., the frequency of the SC spectra distributes in bowlike patterns increases with the increase of the distance between the bowlike pattern and the core of the probe pulse. Diffraction should be accompanied by diffraction patterns with bright and energy-concentration spots in the centers to represent the incident pulse distributions,[39] so the bowlike patterns of the probe pulse are not caused by the diffraction of plasma grating, as no bright and energy-concentration spots are detected in the three bowlike patterns. Filamentation of femtosecond laser pulses can cause an ultrafast refractive index change which is induced by the electronic Kerr effect and the plasma's isotropic medium.[40] Due to the nonlinear interaction between the probe pulse and the plasma grating, the refractive index is redistributed in the interaction area, i.e., a change (increase or decrease) of the local refractive index. The incident pulses change their original propagating directions, are reformed in the high-refractive-index region, and projected in the far-field region as bowlike patterns. However, the bowlike patterns obtained with time delay of −200 fs are more obvious than that obtained with time delay of 200 fs as shown in Figs. 2(c) and 2(g). The multiphoton ionization is introduced to interpret the asymmetrical phenomenon. Compared with the plasma grating, the lifetime of the plasma of the interaction area can be enlarged when the plasma grating interacts with a probe pulse.[37] When tuning the time delay in the positive range to be more than 200 fs, multiphoton ionization begins to dominate the filamentation of the probe pulse to generate ions to keep the survival of the plasma of the interaction area, resulting in the attenuation of the SC generation as shown in Fig. 2(a) and the intensity of the bowlike patterns as shown in Figs. 2(c) and 2(g).

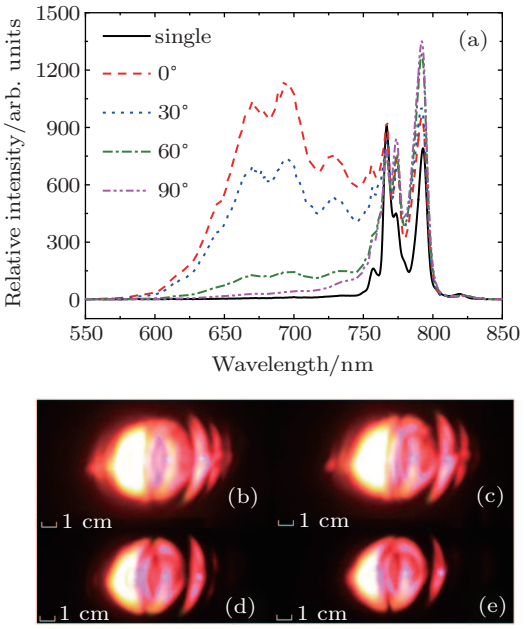


Fig. 3. (color online) (a) Dependence of measured SC spectra on the relative polarization angle between probe pulse and pump pulses, and output spatial profiles of three pulses with different relative polarization angles. (b)–(e) are output spatial profiles with relative polarization angles set to be 0°, 30°, 60°, and 90°, respectively.

The relative polarization angle between the probe pulse and the two pump pulses is changed, and the dependence of the SC spectra of the probe pulse on the relative polarization angle when the time delay set to 0 fs is shown in Fig. 3(a). The spectral width of the SC generation of the probe pulse relates to the relative polarization angle. The output spatial profiles of the three pulses measured with the relative polarization angle between the probe pulse and the pump pulses set to 0°, 30°, 60°, and 90° are shown in Figs. 3(b)–3(d), respectively. The number and the intensity of bowlike patterns of the probe pulse reduce with the increase of relative polarization angle. As is known, the spatiotemporal modulation of the pulses during the filament interaction can be changed by turning the relative polarization angle between them. Therefore,

the cross defocusing condition is changed, resulting in the decrease of the intensity of the SC generation with the increases of relative polarization angle and the SC cutoff wavelength. As the high frequency components of the SC generation are weakened with the increase of relative polarization angle, the number and the intensity of bowlike patterns of the probe pulse are reduced.

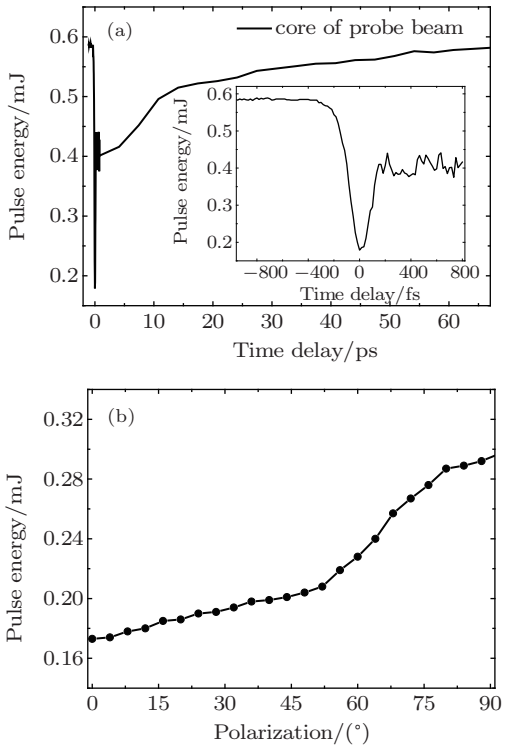


Fig. 4. Dependences of core energy of probe pulse after filamentation on (a) time delay and (b) relative polarization angle between the probe pulse and pump pulses.

In order to further understand the processes involving the probe pulse interacting with the plasma grating, the core energy of probe pulse as functions of the time delay and relative polarization angle between the probe pulse and the pump pulses are shown in Figs. 4(a) and 4(b), respectively. As shown in the inset of Fig. 4(a), the pulse energy begins to decrease when the time delay is tuned to −200 fs and reaches a minimum of about 0.16 mJ when the time delay is tuned to 0 fs, and then radically increase to an approximate constant of 0.4 mJ when the time delay is tuned to 200 fs. The dominant nonlinear process is filament-interaction-induced laser defocusing, which releases energy from the filament core to the reservoir. The value of the core energy of the probe pulse exhibits an irregular oscillation with the time delay when the time delay is changed in the range from 200 fs to 15 ps, and this phenomenon is only shown by the inset figure from 200 fs to 800 fs. Then the pulse energy increases slowly with the time delay as the time delay is changed in the time range larger than 15 ps. In order to keep the survival of the plasma in the interaction area, part of the probe pulse energy transfers to the plasma generation. There is an energy competition between the survival of the plasma of the interaction area and the filamentation of the probe pulse, resulting in the irregular oscillation in the time range from 200 fs to 15 ps. When the time delay is tuned to 60 ps, the filamentation of the probe pulse wins the competition, and nearly no energy of the probe pulse transfers to the plasma generation of plasma grating, which induces the death of the plasma grating. As to how the core energy of the probe pulse changes with the relative polarization angle with the time delay set to 0 fs. The core energy of the probe pulse increases with the increase of relative polarization angle between the probe pulse and the pump pulses, i.e., the energy lose to SC generation decreases with the increase of the polarization angle, which is in good agreement with the observations in Fig. 3.

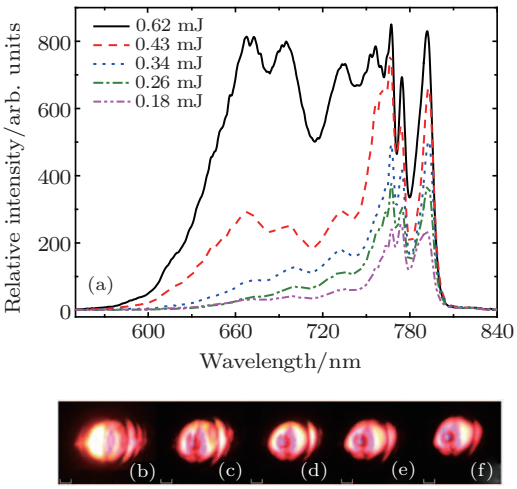


Fig. 5. (color online) (a) Dependence of measured SC spectra on input probe pulse energy, and output spatial profiles of three pulses. (b)–(f) are output spatial profiles with input probe pulse energy set to 0.62 mJ, 0.43 mJ, 0.34 mJ, 0.26 mJ, and 0.18 mJ, respectively.

The input probe pulse energy is changed from 0.18 mJ to 0.62 mJ when the time delay is fixed to 0 fs, the SC spectra and the far-field spatial profiles of the three pulses are measured. Figure 5(a) shows the SC spectra measured with different probe pulse energy, and figures. 5(b)–5(f) show the output spatial profiles corresponding to probe pulse energies of 0.62 mJ, 0.43 mJ, 0.34 mJ, 0.26 mJ, and 0.18 mJ, respectively. It is clear that the intensity and spectral width reduce with the decrease of the input probe pulse energy, because the self-phase modulation and self-steepening effect are weakened when the input probe pulse energy is decreased. As a result, the number and intensity of bowlike patterns of the probe filament reduce with a decrease of the input probe pulse energy. The dependence of the core energy ratio of the probe pulse on the input probe pulse energy when the time delay set to 0 fs is shown in Fig. 6, and the core energy ratio is defined as the core energy of probe pulse after interacting with the plasma grating divided by its input pulse energy. Compared

with losing 50% of the probe pulse energy to the SC generation when the input probe pulse energy is 0.18 mJ, 71% energy lost to the SC generation when the input probe pulse energy is 0.62 mJ, which means less energy is lost to the SC generation with smaller probe pulse energy impacting on the plasma grating. The dependence of the core energy ratio on the input probe pulse energy demonstrates that the high-energy probe laser pulse makes much more drastic competition among nonlinear processes than the low-energy probe pulse.

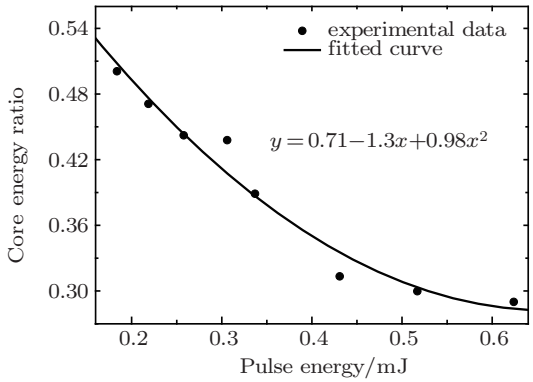


Fig. 6. Dependence of core energy ratio of the probe pulse on input probe pulse energy.

4. Conclusion

In summary, the spectral modulation and SC generation of a probe pulse crossing a plasma grating with a small crossing angle is investigated in this paper. The SC generation from the probe pulse and the core energy of the probe pulse after filamentation strongly depend on the time delay, the relative polarization angle between the probe pulse and the pump pulses, and the input probe pulse energy. The cross defocusing effect induces the broadening of the SC generation. The output spatial profiles of the three pulses are shown, and the detected bowlike patterns are proved to be caused by the change of refractive index in the interaction area. The dependences of the core energy of the probe pulse on the time delay and relative polarization angle are in good agreement with those of the SC generation and the output spatial profiles of the probe pulse on the two parameters.

References

[1] Couairon A and Mysyrowicz A 2007 *Phys. Rep.* **411** 47
[2] Zhang X P, Jiang H B, Chen L, Jiang Y Y, Yang H and Gong Q H 2010 *Chin. Phys. B* **19** 034209
[3] Hao Z Q, Zhang J, Lu X, Xi T T, Yuan X H, Zheng Z Y, Lu X, Yu M Y, Li Y T, Wang Z H, Zhao W and Wei Z Y 2007 *Opt. Express* **15** 16102
[4] Panagiotopoulos P, Efremidis N K, Papazoglou D G, Couairon A and Tzortzakis S 2010 *Phys. Rev. A* **82** 061803
[5] Sun H Y, Luo F F, He F, Liao Y and Xu J 2010 *Chin. Phys. B* **19** 054210
[6] Hauri C P, Kornelis W, Helbing F W, Heinrich A, Couairon A, Mysyrowicz A, Biegert J and Keller U 2004 *Appl. Phys. B* **79** 673
[7] Couairon A, Franco M, Mysyrowicz A, Biegert J and Keller U 2005 *Opt. Lett.* **30** 2657
[8] Couairon A, Biegert J, Hauri C P, Kornelis W, Helbing F W, Keller U and Mysyrowicz A 2006 *J. Mod. Opt.* **53** 75
[9] Zair A, Guandalini A, Schapper F, Holler M, Biegert J, Gallmann L, Couairon A, Franco M, Mysyrowicz A and Keller U 2007 *Opt. Express* **15** 5394
[10] Chen X W, Zeng Z N, Dai J, Li X F, Li R X and Xu Z Z 2008 *Chin. Phys. B* **17** 1826
[11] Mysyrowicz A, Couairon A and Keller U 2008 *New J. Phys.* **10** 025023
[12] Li Y T, Wang W M, Li C and Sheng Z M 2012 *Chin. Phys. B* **21** 095203
[13] Wang T J, Daigle J F, Chen Y, Marceau C, Theberge F, Chateauneuf M, Dubois J and Chin S L 2010 *Laser Phys. Lett.* **7** 517
[14] Wu L, Ling F R, Zuo Z G, Liu J S and Yao J Q 2012 *Chin. Phys. B* **21** 017802
[15] Ganeev R A, Suzuki M, Baba M, Kuroda H and Kulagin I A 2006 *Appl. Opt.* **45** 748
[16] Yang H, Zhang J, Zhao L Z, Li Y J, Teng H, Li Y T, Wang Z H, Chen Z L, Wei Z Y, Ma J X, Yu W and Sheng Z M 2003 *Phys. Rev. E* **67** 015401
[17] Liu Z Y, Lu X, Liu Q C, Sun S H, Li L, Liu X L, Ding B W and Hu B T 2012 *Appl. Phys. B* **108** 493
[18] Liu J S, Schroeder H, Chin S L, Li R X and Xu Z Z 2005 *Opt. Express* **13** 10248
[19] Wu J, Cai H, Peng Y, Tong Y Q, Couairon A and Zeng H P 2009 *Laser Phys.* **19** 1759
[20] Wu J, Cai H, Couairon A and Zeng H P 2009 *Phys. Rev. A* **80** 013828
[21] Cai H, Wu J, Bai X S, Pan H F and Zeng H P 2010 *Opt. Lett.* **35** 49
[22] Cai H, Wu J, Peng Y, Pan H F and Zeng H P 2009 *Opt. Express* **17** 5822
[23] Wang Y D, Zhang Y S, Chen P, Shi L P, Lu X, Wu J, Ding L E and Zeng H P 2011 *Appl. Phys. Lett.* **98** 111103
[24] Kasparian J, Rodriguez M, Mejean G, Yu J, Salmon E, Wille H, Bourayou R, Frey S, Andre Y B, Mysyrowicz A, Sauerbrey R, Wolf J P and Woste L 2003 *Science* **301** 61
[25] Xu H, Ejean G M, Liu W, Kamali Y, Daigle J F, Azarm A, Simard P T, Mathieu P, Roy G, Simard J R and Chin S L 2007 *Appl. Phys. B* **87** 151
[26] Liu Y, Durand M, Chen S, Houard A, Prade B, Forestier B and Mysyrowicz A 2010 *Phys. Rev. Lett.* **105** 055003
[27] Yang X, Wu J, Tong Y Q, Ding L E, Xu Z Z and Zeng H P 2010 *Appl. Phys. Lett.* **97** 071108
[28] Shi L P, Li W X, Wang Y D, Lu X, Ding L E and Zeng H P 2011 *Phys. Rev. Lett.* **107** 095004
[29] Polynkin P, Kolesik M and Moloney J V 2009 *Phys. Rev. Lett.* **103** 123902
[30] Polynkin P, Kolesik M, Moloney J V, Siviloglou G A and Christodoulides D N 2009 *Science* **324** 229
[31] Varma S, Chen Y H and Milchberg H M 2008 *Phys. Rev. Lett.* **101** 205001
[32] Yang X, Wu J, Peng Y, Tong Y Q, Lu P F, Ding L E, Xu Z Z and Zeng H P 2009 *Opt. Lett.* **34** 24
[33] Liu J, Li W X, Pan H F and Zeng H P 2011 *Appl. Phys. Lett.* **99** 151105
[34] Kiran P P, Bagchi S, Arnold C L, Krishnan S R, Kumar G R and Couairon A 2010 *Opt. Express* **18** 21504
[35] Kosareva O G, Liu W, Panov N A, Bernhardt J, Ji Z, Sharifi M, Li R X, Xu Z Z, Liu J S, Wang Z, Ju J, Lu X, Jiang Y, Leng Y, Liang X, Kandidov V P and Chin S L 2009 *Laser Phys.* **19** 1776
[36] Kiran P P, Bagchi S, Krishnan S R, Arnold C L, Kumar G R and Couairon A 2010 *Phys. Rev. A* **82** 013805
[37] Liu Z Y, Ding P J, Shi Y C, Lu X, Sun S H, Liu X L, Liu Q C, Ding B W and Hu B T 2012 *Opt. Express* **20** 8837
[38] Akozbek N, Trushin S A, Baltuska A, Fu W, Goulielmakis E, Kosma K, Krausz F, Panja S, Uiberacker M, Schmid W E, Becker A and ScaloraMand Bloemer M 2006 *New J. Phys.* **8** 177
[39] Yang X, Wu J, Peng Y, Tong Y Q, Lu P F, Ding L E, Xu Z Z and Zeng H P 2009 *Opt. Lett.* **34** 3806
[40] Marceau C, Ramakrishna S, Genier S, Wang T J, Chen Y P, Theberge F, Chateauneuf M, Dubois J, Seideman T and Chin S L 2010 *Opt. Commun.* **283** 2732